Physics of the Earth and Planetary Interiors 168 (2008) 97–102

Contents lists available at ScienceDirect

Physics of the Earth and Planetary Interiors

journal homepage: www.elsevier.com/locate/pepi

Effect of Fe on the equation of state of mantle silicate perovskite over 1 Mbar

S. Lundin[a,1], K. Catalli[a], J. Santillán[a,2], S.-H. Shim[a,*], V.B. Prakapenka[b], M. Kunz[c], Y. Meng[d]

[a] Department of Earth, Atmospheric, and Planetary Sciences, Massachusetts Institute of Technology, MA, USA
[b] GeoSoilEnviroCARS, University of Chicago, IL, USA
[c] Advanced Light Source, Lawrence-Berkeley National Laboratory, CA, USA
[d] HPCAT, Advanced Photon Source, Argonne National Laboratory, IL, USA

ARTICLE INFO

Article history:
Received 15 January 2008
Received in revised form 29 April 2008
Accepted 9 May 2008

Keywords:
Perovskite
Equation of state
Spin transition
X-ray diffraction
Mantle

ABSTRACT

In order to investigate the effect of Fe on the equation of state (EOS), the volume of the perovskite (Pv) phases, $(Mg_{1-x}Fe_x)SiO_3$, with different Fe contents ($x = 0$, 0.09, 0.15), has been measured at high pressures up to 1 Mbar in an Ar or NaCl medium. A bulk modulus (K_0) ranging between 255 and 261 GPa is obtained when the Au scales consistent with the Pt scale are used and the data are fit to the second order Birch–Murnaghan (BM) equation. When the third order BM equation is used, we obtain $K_0 = 250$–264 GPa and $K_0' = 3.7$–4.5, which is consistent with previous low-pressure X-ray diffraction and Brillouin measurements. Within experimental uncertainties (0.5% in volume and 6% in bulk modulus), we do not resolve differences in the EOS between Fe-bearing (up to 15%) and Fe-free Pv to 1 Mbar (2600-km depth in the mantle). This is in contrast with the much larger effect of the Fe spin transition for the EOS of ferropericlase (Fp) reported recently. This is perhaps due to much more diverse states of Fe (e.g., oxidation, coordination, and spin states) in Pv than in Fp.

1. Introduction

Iron is the most abundant transition metal in the mantle and enters the crystal structures of the dominant mantle phases, silicate perovskite (Pv) and ferropericlase (Fp) (e.g., Kesson et al., 1998). The effect of Fe on the equation of state (EOS) of these mantle phases is fundamental for constraining the chemical composition of the lower mantle combined with seismic models (Stixrude et al., 1992).

It has been predicted that Fe in the mantle phases undergoes a magnetic collapse at pressure relevant for the lower mantle (Cohen et al., 1997). Recent spectroscopic measurements have found that the spin state of Fe in Pv and Fp changes at mantle pressures (Badro et al., 2003, 2004; Li et al., 2004; Speziale et al., 2005; Jackson et al., 2005). Moreover, the spin transition in Fp affects the pressure (P)–volume (V) relations (Lin et al., 2005; Speziale et al., 2005; Fei et al., 2007), which has been further supported by first-principles calculations (Tsuchiya et al., 2006; Persson et al., 2006).

However, no systematic EOS measurements have been performed for Pv, which is the dominant phase in the lower mantle, by varying the content of Fe at mantle pressures. An earlier study (Mao et al., 1991) investigated the effect of Fe and concluded that Fe does not change the EOS of Pv. Yet the data were collected only up to 29 GPa which is much lower than the reported spin transition pressure in Pv, 70–120 GPa (Badro et al., 2004; Li et al., 2004). Although the EOS of Pv with different Fe contents have been measured to higher pressures by some investigators (e.g., Knittle and Jeanloz, 1987), it is difficult to reliably extract the effect of Fe by combining these data, because of the use of different pressure scales and pressure transmitting media in these measurements. Furthermore, even for the Pv phase in $MgSiO_3$, the most studied system, P–V relations have been measured without pressure medium above 50 GPa. Therefore, it is necessary to investigate the effect of Fe on Pv at mantle pressures under improved stress conditions using the same pressure scale in order to facilitate comparison among the Pv phases with different Fe contents.

First-principles studies (Zhang and Oganov, 2006; Stackhouse et al., 2007) and experimental measurements (Badro et al., 2004; Li et al., 2004; Jackson et al., 2005) are in agreement in that the spin transition occurs over a wide pressure range in Pv. Also the computational studies have suggested that the transition occurs gradually in Pv. In other words, if the spin transition indeed affects density of Pv, it likely happens gradually over a wide pressure range. Therefore, the effect of the spin transition may be recognized from differences in compressibility between Fe-bearing and Fe-free Pv, rather than by a discrete change (or a change over a narrow P range)

* Corresponding author. Present address: 77 Massachusetts Avenue 54-616, Cambridge, MA 02139, USA. Tel.: +1 617 324 0249.
E-mail address: sangshim@mit.edu (S.-H. Shim).
[1] Present address: Ocean Surveys, INC, RI, USA.
[2] Present address: Ahura Corporation, MA, USA.

0031-9201/$ – see front matter © 2008 Elsevier B.V. All rights reserved.
doi:10.1016/j.pepi.2008.05.002

in density as found in Fp (Lin et al., 2005; Speziale et al., 2005; Fei et al., 2007).

We report the P–V relations of $(Mg_{1-x}Fe_x)SiO_3$-Pv ($x = 0$, 0.09, 0.15) over 1 Mbar. In order to resolve differences in the EOS among different composition systems, we use the same pressure scale (Au) throughout the measurements and the same pressure medium (Ar) for most of the data up to 1 Mbar.

2. Experimental methods

Natural pyroxene samples [$(Mg_{1-x}Fe_x)SiO_3$] with $x = 0.00$, 0.09, and 0.15 are used as starting materials. The chemical compositions of the samples were examined using electron microprobe at MIT. No significant amounts of other minor elements are detected for the starting materials. The starting materials were ground to powders and mixed with 10 wt% Au which serves as an internal pressure standard and laser coupler. The mixtures were pressed to 5-μm thick foils. Each foil was loaded in a hole in a preindented Re gasket and then the assemblage was sandwiched between diamond anvils in a symmetric type diamond-anvil cell. For most of our measurements, we cryogenically loaded Ar as a pressure transmitting and insulation medium in the sample chamber. A few grains of the sample materials were placed below and above the sample foil in order to allow liquid Ar to flow in between the foil and diamond anvils. The diffraction lines of Ar are well resolved up to our maximum pressure, confirming that a significant amount of the pressure medium surrounds our samples (Fig. 1). In some measurements for the sample with $x_{Fe} = 9$ mol%, a sample foil was sandwiched between two foils of NaCl which serves as an insulation and pressure medium.

We used a culet size of 200 μm for measurements up to 80 GPa. Beveled anvils with 150 μm culets were used for measurements at pressures above 80 GPa. In order to examine reproducibility, we conducted at least 3 different runs for each compositional system with pressure ranges overlapping at least 10 GPa.

X-ray diffraction (XRD) measurements were conducted at the GSECARS sector and the HPCAT beamline of Advanced Photon Source (APS) and the 12.2.2 beamline of Advanced Light Source (ALS). A monochromatic X-ray beam with an energy of 30 keV was focused to a size smaller than 10 μm × 20 μm. Two-dimensional diffraction images were collected using a Mar345 imaging plate or a MarCCD detector. Diffracted beams were measured through X-ray semi-transparent (40–60% transmittance for a 30-keV X-ray beam) cBN backing plates, which extends measurable d-spacings to 1.1 Å. This is particularly helpful for accurate determination of volume for Pv and Au. A total of 9–25 diffraction lines are used to constrain the volume of Pv. For Au, we use 3–5 diffraction lines.

In order to synthesize the Pv phases, the sample in the diamond-anvil cell was heated with an Nd:YLF laser beam to 1500–2000 K at pressures higher than 35 GPa for at least 20 min. Laser heating was conducted at MIT, APS, and ALS. The samples were also scanned with the laser before each diffraction measurement in order to anneal the deviatoric stresses.

One of the key requirements for the determination of EOS is the accuracy of the pressure scale. Recent studies have shown that the popular X-ray pressure scales, such as Pt, Au, and MgO, are not consistent with each other (Irifune et al., 1998; Shim et al., 2001a; Fei et al., 2004; Dewaele et al., 2004; Hirose et al., 2006). Although less discrepancy exists among the different Pt scales (Jamieson et al., 1982; Holmes et al., 1989), the existing Pt scales are constrained only by shock-wave measurements in which the temperature effect is difficult to separate. The EOS of Au has been much more extensively studied (e.g., Takemura, 2001; Shim et al., 2002; Dewaele et al., 2004; Tsuchiya, 2003; Akahama et al., 2002; Fei et al., 2004). However, the existing Au scales predict pressures that differ by as much as 20 GPa at 1.2 Mbar. Yet, as pointed out by Jamieson et al. (1982), Au is preferred to Pt as a pressure scale due to its higher compressibility. In addition, Au can couple with infrared laser beams for heating like Pt. In this study, we use the Au scales (Tsuchiya, 2003; Dewaele et al., 2004) which are known to be more consistent with the Pt scales (Jamieson et al., 1982; Holmes et al., 1989) in order to facilitate the comparison of our data with previous X-ray studies as most of them used the Pt scales.

3. Result

In order to synthesize the Pv phase at the stable P–T conditions, we compressed the starting materials directly to 35–50 GPa. Synthesis of the Pv phase was confirmed during or after heating at 2000 K (Fig. 1). The diffraction lines from the Pv phase are fit well to an orthorhombic unit cell (space group: *Pbnm*). The Pv phase was observed up to 108 GPa, confirming its stability in the lower mantle (Knittle and Jeanloz, 1987; Serghiou et al., 1998; Shim et al., 2001b).

The postperovskite (PPv) transition has been reported at 100–120 GPa in $(Mg,Fe)SiO_3$ (Murakami et al., 2004; Mao et al., 2005; Shieh et al., 2006; Hirose et al., 2006; Shim et al., 2008). Furthermore, it has been shown that Fe does not partition into Pv and PPv with equal amounts (Murakami et al., 2005; Kobayashi et al., 2005). Therefore, we exclude data points with any sign of the PPv transition. It is notable that in our measurements on $x_{Fe} = 15$ mol% the PPv transition was detected above 110 GPa after heating. If thermal pressure is included, the transition pressure would be approximately 120 GPa, which is more consistent with a small effect of Fe on the PPv transition as reported by Hirose et al. (2006).

For some samples, we observed a weak diffraction line at 2.6–2.8 Å which has been also documented in previous measurements (e.g., O'Neill and Jeanloz, 1994). In diffraction images, the line consists of only a few dots indicating that the diffraction line is from a highly preferred oriented phase. This line can be assigned to the most intense line of stishovite (or $CaCl_2$-type SiO_2), although it is the only line that can be uniquely assigned to SiO_2. If the appearance of SiO_2 would be a result of $(Mg,Fe)SiO_3 \rightarrow (Mg,Fe)O + SiO_2$, we should have seen lines from Fp. However, we did not observe any lines that can be exclusively assigned to Fp.

This line was more frequently observed in the Fe-bearing samples. McCammon (1997) reported that significant amount of Fe is Fe^{3+} in $(Mg,Fe)SiO_3$-Pv synthesized from Fe^{3+}-free starting materials. Frost et al. (2004) proposed that Fe^{3+} in $(Mg,Fe)SiO_3$-Pv is due to a charge disproportionation ($3Fe^{2+} \rightarrow 2Fe^{3+} + Fe^0$). Therefore, some amount of SiO_2 could form through this reaction. However, we could not detect any line which can be assigned to metallic Fe.

This line was also observed in one of the two different samples of Mg endmember, although the intensity is very low (Fig. 1b). The Pv phase in Fig. 1b was synthesized at 42 GPa. When it was synthesized, we found the 2.8 Å peak. Therefore, the peak observed at 89 GPa can be from a small amount of SiO_2 formed during synthesis at low pressure. However, in the run where Pv was first synthesized at 78 GPa, we did not observe the 2.8 Å peak.

In a separate run, we first synthesized pure Pv without the 2.8 Å line at 54 GPa (Fig. 1a) and then heated while the sample was decompressed. The 2.8 Å peak appeared when the sample was heated at 25 GPa. This observation may indicate that SiO_2 may form below 42 GPa in $MgSiO_3$. If this is the case, $MgSiO_3$-Pv synthesized at low pressure may have some amount of defects in the structure. Interestingly, the P–V relation measured during the decompression is distinct from that at higher pressures. This could also be due to the fact that we did not anneal the sample during decompression in order to prevent back transformation to low-pressure phases.

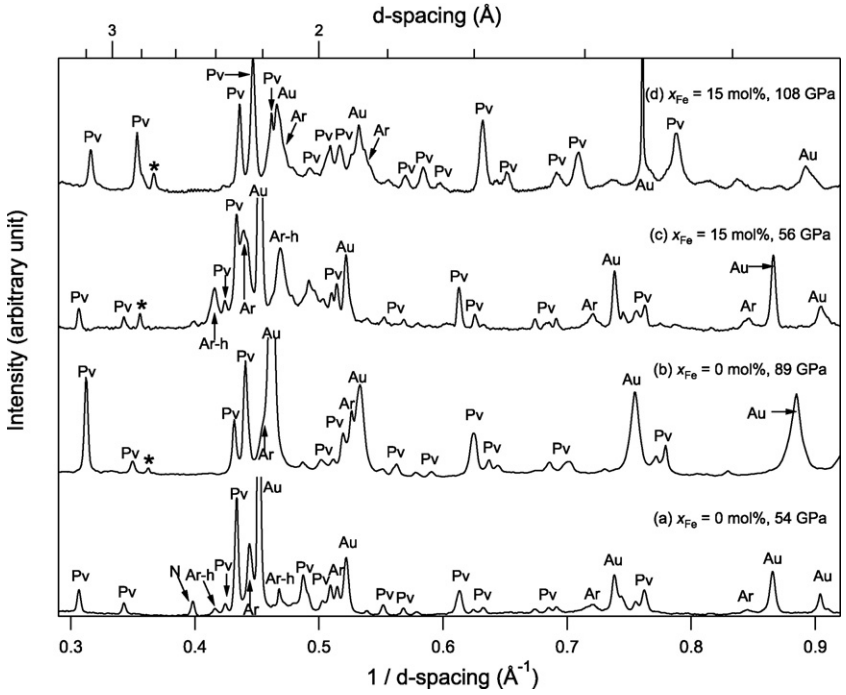

Fig. 1. X-ray diffraction patterns of (Mg,Fe)SiO_3 perovskites at high pressure and room temperature. The backgrounds are subtracted from the patterns. Identifications for the main diffraction lines are provided with labels (Pv: perovskite, Au: gold pressure standard, Ar: argon pressure medium, Ar-h: the hcp phase of Ar, N: nitrogen, and ∗: unknown).

Therefore, we do not include the decompression data for EOS fit. However, at pressures higher than 40 GPa, the volume of $MgSiO_3$-Pv in the sample with the 2.8 Å peak agrees well with that in the sample without the 2.8 Å peak. Therefore, this might indicate that the defects are removed from the structure when the Pv phase is further heated at higher pressures. Also it should not be ruled out that small amount of SiO_2 (possibly as inclusions) may exist in our natural starting materials.

In some samples, we found a few diffraction lines which can be assigned to the hexagonal closed-packed (hcp) phase of Ar which was loaded as a pressure medium. Ar is stable in a face-centered cubic (fcc) structure up to 50 GPa and then gradually transforms to an hcp phase (Errandonea et al., 2006). In most of the diffraction patterns where we find hcp-Ar, we also observe a weak line which can be assigned to a high-pressure polymorph of nitrogen (Gregoryanz et al., 2007). The existence of nitrogen is further confirmed by Raman spectroscopy. The small amount of nitrogen is perhaps captured during cryogenic loading of Ar. It is known that the existence of small amounts of nitrogen can stabilize the hcp phase of Ar (Wittlinger et al., 1997).

We fit the measured P–V relations of different compositional systems to the second and third order Birch–Murnaghan (BM) equations with weights calculated from the uncertainties in P and V (Table 1 and Fig. 2). Because a severe correlation exists between bulk modulus, K_0, and its pressure derivative, $K_0' = (dK/dP)_{P=0}$, in the fitting (Bell et al., 1987), fixing $K_0' = 4$ during the fitting (i.e., second order BM equation) provides a simpler comparison. Using the Au scales by Dewaele et al. (2004) and Tsuchiya (2003), we obtained K_0 = 255–257 and 259–261 GPa, respectively (Fig. 2). However, no clear effect of Fe on the compressibility of Pv is resolved within the experimental uncertainty.

Our K_0 values obtained with these Au scales are consistent with previous XRD measurements (253–266 GPa) (e.g., Knittle and Jeanloz, 1987; Mao et al., 1991; Fiquet et al., 2000; Vanpeteghem et al., 2006) and Brillouin spectroscopy (253–264 GPa) (Yeganeh-Haeri, 1994; Sinogeikin et al., 2004). The fact that our results with the Au scales by Dewaele et al. (2004) and Tsuchiya (2003) agree well with the previous results (Fiquet et al., 2000) with the Pt scale by Holmes et al. (1989) confirms the previous reports (Akahama et al., 2002; Dewaele et al., 2004) that these two Au scales are in agreement with the Pt scale. However, these Pt scales are constrained only by shock-wave measurements. The consistency does not necessarily mean the accuracy of the pressure scales. More work is warranted to enhance the accuracy of the important pressure scales.

Table 1
The volumes of (Mg,Fe)SiO_3 perovskites at high pressure and 300 K used for equation of state fits

x_{Fe} = 0 mol%		x_{Fe} = 9 mol%		x_{Fe} = 15 mol%	
P (GPa)	V (Å^3)	P (GPa)	V (Å^3)	P (GPa)	V (Å^3)
28.8(6)	147.96(3)	1 bar	163.18(3)	1 bar	163.30(7)
30.3(6)	147.06(4)	36.2(7)	145.81(3)	30.3(4)	148.48(5)
36.0(8)	144.95(3)	36.9(5)	145.80(6)	39.4(6)	144.41(8)
37.1(8)	144.83(3)	39.0(5)	145.11(6)*	42.2(8)	143.93(13)
42.0(9)	142.90(3)	45.0(6)	142.72(3)	44.7(7)	143.16(9)
42.1(9)	143.19(3)	46.5(9)	142.26(3)	48.2(10)	141.61(5)
46.1(10)	141.24(3)	49.3(7)	141.42(6)	52.9(8)	140.66(4)
48.5(11)	140.93(3)	51.5(7)	140.63(4)	56.2(9)	139.56(7)
49.5(11)	140.46(3)	54.4(11)	140.02(5)*	58.0(9)	139.13(2)
54.2(13)	139.36(3)	55.2(9)	139.85(5)	59.1(10)	138.28(9)
56.7(14)	138.74(3)	56.0(9)	139.26(3)	64.6(11)	136.88(9)
68.5(17)	135.75(3)	56.2(9)	139.32(5)	71.0(12)	135.19(14)
73.3(25)	134.12(4)	60.4(10)	137.94(4)	79.3(14)	132.89(14)
80.2(21)	133.05(3)	64.6(7)	137.06(4)*	84.7(15)	131.75(13)
88.5(24)	131.07(3)	64.7(11)	136.91(6)	92.9(20)	130.47(13)
93.0(5)	129.61(3)	80.6(9)	132.63(5)*	95.9(18)	129.66(19)
		86.1(20)	131.01(7)*	107.9(21)	127.49(15)

Pressure is calculated using the Au scale by Tsuchiya (2003). The numbers in the parentheses are 1σ uncertainties. The data points with ∗ were obtained in a NaCl pressure medium. All other data points were obtained in an Ar pressure medium.

Some interesting trends can be found in the third order fit results (Fig. 2): K_0' is lower in Fe-bearing than Fe-free Pv, regardless of the pressure scale used. For $x_{Fe} = 9$ mol% in particular, the low K_0' is strongly influenced by the data points existing between 80 and 90 GPa (Fig. 2b). Indeed, these two data points lie on the compressional curve of Mg-endmember.

For more investigation, we calculate the volume difference, $\Delta V/V = (V_{FePv} - V_{Pv})/V_{Pv}$, between Fe-bearing ($V_{FePv}$) and Fe-free ($V_{Pv}$) Pv for each data point using the third order BM equation fit results for Fe-free Pv (Fig. 3 a). It can be seen that the $\Delta V/V$ of Pv in $x_{Fe} = 9$ mol% decreases with P and its volume becomes indistinguishable from that of Mg-endmember at 80 GPa. For $x_{Fe} = 15$ mol%, a similar gradual decrease in $\Delta V/V$ with pressure can be seen to 80 GPa. Then the $\Delta V/V$ above 80 GPa appears to increase to a value similar to that at 1 bar. Interestingly, the subtle changes in volume behaviors are observed at the pressure range where partial spin pairing has been reported in spectroscopy measurements (Badro et al., 2004).

We also calculated density differences ($\Delta\rho/\rho$) between Fe-bearing and Fe-free Pv in the same fashion (Fig. 3b). A decrease in $\Delta V/V$ would result in an increase in the density of Fe-bearing Pv over the pressure range, as it can be seen at 80–90 GPa in both $x_{Fe} = 9$ mol% and $x_{Fe} = 15$ mol%.

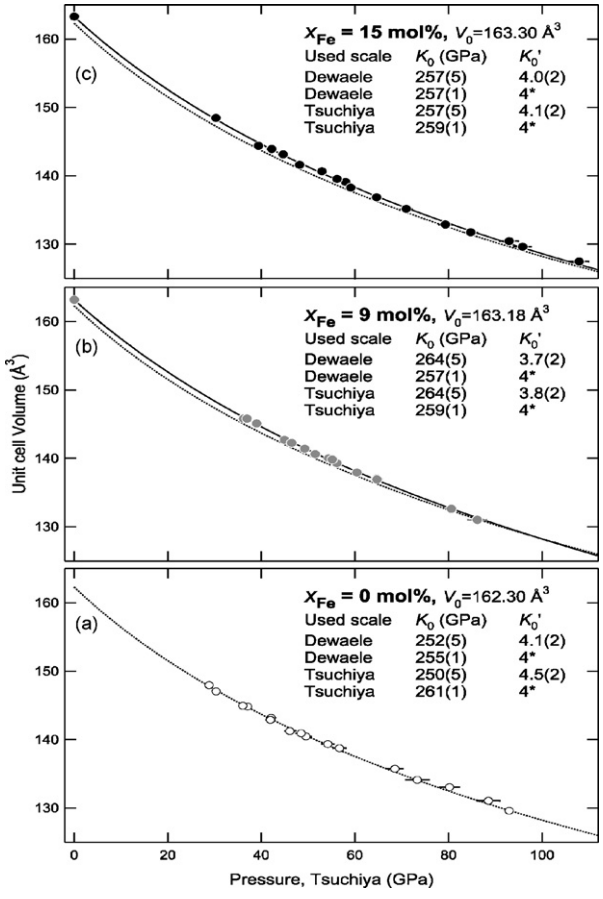

Fig. 2. P–V equations of state of (Mg,Fe)SiO_3 perovskites over 1 Mbar. Results for the fitting to the second and third order Birch–Murnaghan equation are shown for the different Au pressure scales. The Au scale by Tsuchiya (2003) is used for presentation of the data points. The dotted line is the fitting results for $MgSiO_3$-Pv data to the third order BM equation. The solid lines in (b) and (c) represent the fitting results for $(Mg_{0.91}Fe_{0.09})SiO_3$- and $(Mg_{0.85}Fe_{0.15})SiO_3$-Pv, respectively. The V_0 of Mg-endmember is obtained from Fiquet et al. (2000). The numbers in the parentheses and the error bars are 1σuncertainties. The fixed parameters are noted with $*$.

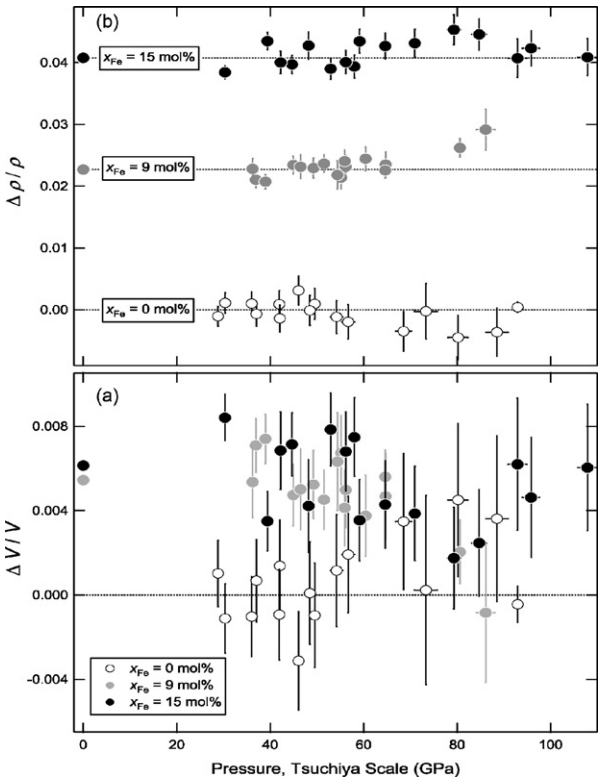

Fig. 3. (a) Volume difference ($\Delta V/V$) and (b) density difference ($\Delta\rho/\rho$) between the Fe-bearing and Fe-free perovskites at high pressure. The effect of compression is removed by subtracting the expected volume from the third order Birch–Murnaghan EOS fit for Mg-endmember. The error bars are the 1σ uncertainties which include uncertainties in volume and the EOS of Mg endmember. The dotted horizontal lines in (b) represent density differences at 0 GPa.

In order to investigate the effect of Fe on the crystal structure of Pv we plot the normalized pseudo-cubic unit-cell axes and their ratios as a function of pressure and composition (Fig. 4). We observe a decrease in anisotropy of the unit cell with an increase of Fe: the b/a and c/a ratios decrease with Fe by 0.2% and 0.3%, respectively (Fig. 4b). As shown in Fig. 4 a, Fe expands the a-axis by 0.2% whereas it shrinks the c-axis by 0.1%. However, no significant effect of Fe can be found for the b-axis.

4. Discussion and summary

The EOS of (Mg,Fe)SiO_3 perovskite (Pv) measured over 1 Mbar using the Au scales (Tsuchiya, 2003; Dewaele et al., 2004) under improved stress conditions confirms the results from previous XRD (Knittle and Jeanloz, 1987; Mao et al., 1991; Fiquet et al., 2000) and Brillouin spectroscopy (Sinogeikin et al., 2004; Yeganeh-Haeri, 1994) measurements. Our measurements also show that the EOS of Pv does not change with Fe up to $x_{Fe} = 15$ mol% within estimated experimental uncertainties.

In the EOS fit residue we found a subtle yet systematic trend in Fe-bearing Pv: the volume of Fe-bearing Pv approaches that of Fe-free Pv at 80–90 GPa where the spin transition has been reported (Badro et al., 2004). However, the magnitudes of the changes are close to the uncertainties of the data points. For the data points which show the closest volumes to Mg-endmember, it is the smaller a-axis that makes the volume small in $x_{Fe} = 9$ mol% whereas it is the smaller c-axis in $x_{Fe} = 15$ mol%. If the volume of Fe-bearing Pv approaching that of Fe-free Pv indeed results from the spin transition, both systems should show similar behaviors for the unit-cell parameters. Therefore, we conclude that the trend in the fit residue

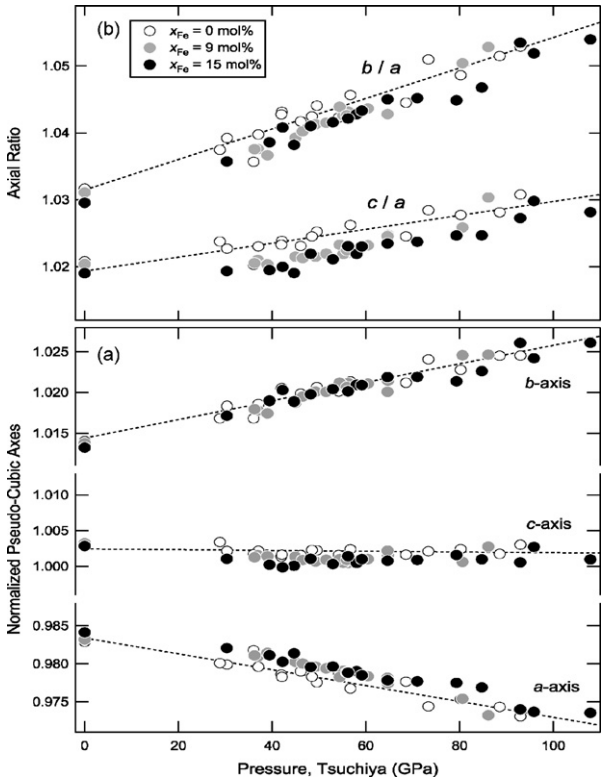

Fig. 4. (a) Normalized pseudo-cubic axes of (Mg,Fe)SiO_3 perovskites ($a^* = a/\sqrt{2} \times (V/4)^{-1/3}$, $b^* = b/\sqrt{2} \times (V/4)^{-1/3}$, and $c^* = c/2 \times (V/4)^{-1/3}$) (Andrault et al., 2007), and (b) ratios between pseudo-cubic axes. The open, grey, and solid circles represent the perovskite phases in $x_{Fe} = 0$ mol%, $x_{Fe} = 9$ mol%, and $x_{Fe} = 15$ mol%, respectively. The data are plotted with respect to the Au scale by Tsuchiya (2003).

of the volume is unlikely significant. In other words, our measurements indicate that the effect of the spin transition on the volume of Pv should not exceed 0.5% in volume or density and 6% in bulk modulus which is the resolution limits of our datasets (Fig. 3).

A much larger effect from the spin transition has been reported for Fp with a mantle-related composition, which is at least a factor of two higher than that expected for Pv, although whether density or compressibility is more sensitive to the electronic transition is under debate: 35% in bulk modulus (Lin et al., 2005) or 4–5% in volume without a significant change in bulk modulus (Speziale et al., 2005; Fei et al., 2007). Also seismic velocity changes (Lin et al., 2006) and elastic anomalies (Crowhurst et al., 2008) have been suggested at the spin transition. This large effect is in sharp contrast with our observations on (Mg,Fe)SiO_3-Pv.

Although it is still unclear whether the electronic transition in Pv occurs stepwise (Badro et al., 2004) or gradually (Li et al., 2004), previous X-ray spectroscopy measurements are in agreement in that the transition occurs over a wide pressure range (~ 50 GPa) in Pv. In contrast, the transition appears to occur over a much more narrow pressure range (~ 15 GPa) in Fp at 300 K (Badro et al., 2003; Lin et al., 2005; Fei et al., 2007), although it is also still under similar debate (Kantor et al., 2006). As pointed out by previous studies (Badro et al., 2004; Li et al., 2004; Jackson et al., 2005), the wider transition pressure range in Pv is perhaps related to the fact that diverse states are available for Fe in Pv: both $Fe^{2+}$and Fe^{3+}exist (McCammon, 1997), two crystallographic sites with different coordination are available for Fe (Horiuchi et al., 1987), and Fe in different oxidation and/or coordination states can have different spin states (Badro et al., 2004).

First-principles studies have shown that Fe^{2+}remains in a high-spin state throughout the mantle (Zhang and Oganov, 2006; Stackhouse et al., 2007). They suggested that Fe^{3+}in the dodecahedral site of Pv would undergo a high- to low-spin transition at 60–80 GPa whereas Fe^{3+}in the octahedral site remains in a low-spin state at all mantle pressures. In addition, Stackhouse et al. (2007) suggested that different Fe–Fe clustering would result in the spin transition occurring at different pressures. Therefore, if a large range of configurations coexist in Pv, which is possible because of small energy differences among the different configurations, the spin transition would appear to occur over a wide range of pressure (Stackhouse et al., 2007).

From these results, we can conclude that the observed subtle effect from the spin transition for the EOS of Pv would be due to the diverse states of Fe. Furthermore, as pointed out by Stackhouse et al. (2007), a relatively low concentration of Fe in Pv compared to that in Fp in the mantle would also be an important factor for the small effect. In fact, Stackhouse et al. (2007) and Bengtson et al. (2007) predicted that the spin transition has only a minor effect on the elastic properties of Pv with a mantle-related composition, consistent with our findings.

Sturhahn et al. (2005) and Tsuchiya et al. (2006) pointed out that high temperature would broaden the pressure range over which the spin transition occurs, which has been experimentally confirmed in Fp (Lin et al., 2007). Therefore, combined with our study, it is likely that the spin transition of Fe in Pv would not result in a significant discontinuity in density or compressibility in the mantle. Furthermore, mantle Pv contains Al and other cations and this would even more diversify the state and configuration of Fe in Pv (Zhang and Oganov, 2006). However, more studies are warranted to explore the effect of the spin transition for other important properties of Pv, such as electrical and optical properties.

Our data also provide some insights on how Fe affects the anisotropy of the Pv structure. Assuming that the SiO_6 octahedra are rigid and regular shaped, the tilting angles of the octahedra can be calculated from the axial ratios of the *Pbnm* Pv (O'Keeffe and Hyde, 1977): $\theta = \cos^{-1}(a/b)$ and $\phi = \cos^{-1}(\sqrt{2}a/c)$. Therefore, the observed smaller axial ratios of Fe-bearing Pv indicate smaller tilting angles of the octahedra. It has been argued that the smaller Mg atom compared with the available size of the dodecahedral site in $MgSiO_3$-Pv may be a cause of the orthorhombic distortion of Pv (Horiuchi et al., 1987). Therefore, the larger size of high-spin (or intermediate spin) Fe (Fei et al., 2007) in the dodecahedral sites would decrease the tilting of the octahedra around them. In addition, the spectroscopy measurements (Badro et al., 2004) have suggested the spin pairing of Fe is not completed until 120 GPa.

Acknowledgements

The discussions with three anonymous reviewers have improved this paper. T.L. Grove provides the starting materials. N. Chatterjee assisted electron microprobe analysis of the starting materials. This work is partly supported by the National Science Foundation (NSF) to Shim (EAR0337005). Portions of this work were performed at the GSECARS and HPCAT sectors of APS, and beamline 12.2.2 of ALS. GSECARS is supported by the NSF and Department of Energy (DOE). HPCAT is supported by DOE-BES, DOE-NNSA, NSF, and the W.M. Keck Foundation. The 12.2.2 beamline is supported by the COMPRES under NSF. Use of APS and ALS is supported by the DOE.

References

Akahama, Y., Kawamura, H., Singh, A.K., 2002. Equation of state of bismuth to 222 GPa and comparison of gold and platinum pressure scales to 145 GPa. J. Appl. Phys. 92, 5892–5897.

Andrault, D., Bolfan-Casanova, N., Bouhifd, M.A., Guignot, N., Kawamoto, T., 2007. The role of Al-defects on the equation of state of Al-(Mg,Fe)SiO_3 perovskite. Earth Planet. Sci. Lett. 263, 167–179.

Badro, J., Fiquet, G., Guyot, F., Rueff, J.P., Struzhkin, V.V., Vanko, G., Monaco, G., 2003. Iron partitioning in Earth's mantle: toward a deep lower mantle discontinuity. Science 300, 789–791.

Badro, J., Rueff, J.-P., Vanko, G., Monaco, G., Fiquet, G., Guyot, F., 2004. Electronic transitions in perovskite: possible nonconvecting layers in the lower mantle. Science 305, 383–386.

Bell, P.M., Mao, H.-K., Xu, J.A., 1987. Error analysis of parameter-fitting in equations of state for mantle minerals. In: Manghnani, M.H., Syono, Y. (Eds.), High-pressure Research in Mineral Physics. Terra Scientific Publication Corporation, pp. 447–454.

Bengtson, A., Persson, K., Morgan, D., 2007. *Ab initio* study of the composition dependence of the pressure-induced spin crossover in perovskite $(Mg_{1-x}Fe_x)SiO_3$. Earth Planet. Sci. Lett. 265, 535–545.

Cohen, R.E., Mazin, I.I., Isaak, D.G., 1997. Magnetic collapse in transition metal oxides at high pressure: implications for the Earth. Science 275, 654–657.

Crowhurst, J.C., Brown, J.M., Goncharov, A.F., Jacobsen, S.D., 2008. Elasticity of (Mg,Fe)O through the spin transition of iron in the lower mantle. Science 319, 451–453.

Dewaele, A., Loubeyre, P., Mezouar, M., 2004. Equations of state of six metals above 94 GPa. Phys. Rev. B 70, 094112.

Errandonea, D., Boehler, R., Japel, S., Mezouar, M., Benedetti, L.R., 2006. Structural transformation of compressed solid Ar: an X-ray diffraction study to 114 GPa. Phys. Rev. B 73, 092106.

Fei, Y., Li, H., Hirose, K., Minarik, W., Van Orman, J., van Westrenen, W., Komabayashi, T., Funakoshi, K., 2004. A critical evaluation of pressure scales at high temperatures by in situ X-ray diffraction measurements. Phys. Earth Planet. Inter. 143–144, 515–526.

Fei, Y., Zhang, L., Corgne, A., Watson, H., Ricolleau, A., Meng, Y., Prakapenka, V.B., 2007. Spin transition and equation of state of (Mg,Fe)O solid solution. Geophys. Res. Lett. 34, 17307.

Fiquet, G., Dewaele, A., Andrault, D., Kunz, M., Le Bihan, T., 2000. Thermoelastic properties and crystal structure of $MgSiO_3$ perovskite at lower mantle pressure and temperature conditions. Geophys. Res. Lett. 27, 21–24.

Frost, D.J., Liebske, C., Langenhorst, F., McCammon, C.A., Trennes, R.G., Rubie, D.C., 2004. Experimental evidence for the existence of iron-rich metal in the Earth's lower mantle. Nature 428, 409–412.

Gregoryanz, E., Goncharov, A.F., Sanloup, C., Somayazulu, M., Mao, H.-K., Hemley, R.J., 2007. High *P–T* transformations of nitrogen to 170 GPa. J. Chem. Phys. 126, 184505.

Hirose, K., Sinmyo, R., Sata, N., Ohishi, Y., 2006. Determination of post-perovskite phase transition boundary in $MgSiO_3$ using Au and MgO pressure standards. Geophys. Res. Lett. 33, 01310.

Holmes, N.C., Moriarty, J.A., Gathers, G.R., Nellis, W.J., 1989. The equation of state of platinum to 660 GPa (6.6 Mbar). J. Appl. Phys. 66, 2962–2967.

Horiuchi, H., Ito, E., Weidner, D.J., 1987. Perovskite-type $MgSiO_3$: single-crystal X-ray diffraction study. Am. Mineral. 72, 357–360.

Irifune, T., Nishiyama, N., Kuroda, K., Inoue, T., Isshiki, M., Utsumi, W., Funakoshi, K.-I., Urakawa, S., Uchida, T., Katsura, T., Ohtaka, O., 1998. The postspinel phase boundary in Mg_2SiO_4 determined by in situ X-ray diffraction. Science 279, 1698–1700.

Jackson, J.M., Sturhahn, W., Shen, G., Zhao, J., Hu, M.Y., Errandonea, D., Bass, J.D., Fei, Y., 2005. A synchrotron Mössbauer spectroscopy study of (Mg,Fe)SiO_3 perovskite up to 120 GPa. Am. Mineral. 90, 199–205.

Jamieson, J.C., Fritz, J.N., Manghnani, M.H., 1982. Pressure measurement at high temperature in X-ray diffraction studies: gold as a primary standard. In: Akimoto, S., Manghnani, M.H. (Eds.), High-pressure Research in Geophysics. Center for Academic Publications Japan, Tokyo, pp. 27–48.

Kantor, I.Y., Dubrovinsky, L.S., McCammon, C.A., 2006. Spin crossover in (Mg,Fe)O: a Mössbauer effect study with an alternative interpretation of X-ray emission spectroscopy data. Phys. Rev. B 73, 100101.

Kesson, S.E., Gerald, J.D.F., Shelley, J.M., 1998. Mineralogy and dynamics of a pyrolite lower mantle. Nature 393, 252–255.

Knittle, E., Jeanloz, R., 1987. Synthesis and equation of state of (Mg,Fe)SiO_3 perovskite to over 100 gigaphascals. Science 235, 668–670.

Kobayashi, Y., Kondo, T., Ohtani, E., Hirao, N., Miyajima, N., Yagi, T., Nagase, T., Kikegawa, T., 2005. Fe–Mg partitioning between (Mg,Fe)SiO_3 post-perovskite, perovskite, and magnesiowüstite in the Earth's lower mantle. Geophys. Res. Lett. 32, L19301.

Li, J., Struzhkin, V.V., Mao, H.-K., Shu, J., Hemley, R.J., Fei, Y., Mysen, B., Dera, P., Prakapenka, V.B., Shen, G., 2004. Electronic spin state of iron in lower mantle perovskite. P. Natl. Acad. Sci. 101, 14027–14030.

Lin, J.-F., Jacobsen, S.D., Sturhahn, W., Jackson, J.M., Zhao, J., Yoo, C.-S., 2006. Sound velocities of ferropericlase in the Earth's lower mantle. Geophys. Res. Lett. 33, L22304.

Lin, J.F., Struzhkin, V.V., Jacobsen, S.D., Hu, M.Y., Chow, P., Kung, J., Liu, H.Z., Mao, H.-K., Hemley, R.J., 2005. Spin transition of iron in magnesiowüstite in the Earth's lower mantle. Nature 436, 377–380.

Lin, J.-F., Vankó, G., Jacobsen, S.D., Iota, V., Struzhkin, V.V., Prakapenka, V.B., Kuznetsov, A., Yoo, C.-S., 2007. Spin transition zone in Earth's lower mantle. Science 317, 1740–1743.

Mao, H.-K., Hemley, R.J., Fei, Y., Shu, J.F., Chen, L.C., Jephcoat, A.P., Wu, Y., 1991. Effect of pressure, temperature, and composition on lattice parameters and density of (Fe,Mg)SiO_3-perovskites to 30 GPa. J. Geophys. Res. 96, 8069–8079.

Mao, W.L., Meng, Y., Shen, G., Prakapenka, V.B., Campbell, A.J., Heinz, D.L., Shu, J.F., Caracas, R., Cohen, R.E., Fei, Y.W., Hemley, R.J., Mao, H.-K., 2005. Iron-rich silicates in the Earth's *D″* layer. P. Natl. Acad. Sci. 102, 9751–9753.

McCammon, C., 1997. Perovskite as a possible sink for ferric iron in the lower mantle. Nature 387, 694–696.

Murakami, M., Hirose, K., Kawamura, K., Sata, N., Ohishi, Y., 2004. Post-perovskite phase transition in $MgSiO_3$. Science 304, 855–858.

Murakami, M., Hirose, K., Sata, N., Ohishi, Y., 2005. Post-perovskite phase transition and mineral chemistry in the pyrolitic lowermost mantle. Geophys. Res. Lett. 32, L03304.

O'Keeffe, M., Hyde, B.G., 1977. Some structure topologically related to cubic perovskite ($e2_1$), ReO_3($d0_9$) and Cu_3Au ($l1_2$). Acta Crystallogr. B33, 3802–3813.

O'Neill, B., Jeanloz, R., 1994. $MgSiO_3$–$FeSiO_3$–Al_2O_3 in the earth's lower mantle—perovskite and garnet at 1200-km depth. J. Geophys. Res. 99, 19901–19915.

Persson, K., Bengtson, A., Ceder, G., Morgan, D., 2006. *Ab initio* study of the composition dependence of the pressure-induced spin transition in the $(Mg_{1-x}Fe_x)O$ system. Geophys. Res. Lett. 33, L16306.

Serghiou, G., Zerr, A., Boehler, R., 1998. (Mg,Fe)SiO_3-perovskite stability under lower mantle conditions. Science 280, 2093–2095.

Shieh, S.R., Duffy, T.S., Kubo, A., Shen, G., Prakapenka, V.B., Sata, N., Hirose, K., Ohishi, Y., 2006. Equation of state of the post-perovskite phase synthesized from a natural (Mg,Fe)SiO_3 orthopyroxene. P. Natl. Acad. Sci. 103, 3039–3043.

Shim, S.-H., Catalli, K., Hustoft, J., Kubo, A., Prakapenka, V.B., Caldwell, W.A., Kunz, M. Crystal structure and thermoelastic properties of $(Mg_{0.91}Fe_{0.09})SiO_3$ postperovskite up to 135 GPa and 2700 K. P. Natl. Acad. Sci. 105, 7382–7386.

Shim, S.-H., Duffy, T.S., Shen, G., 2001a. The post-spinel transformation in Mg_2SiO_4 and its relation to the 660-km seismic discontinuity. Nature 411, 571–574.

Shim, S.-H., Duffy, T.S., Shen, G., 2001b. Stability and structure of $MgSiO_3$ perovskite to 2300-km depth conditions. Science 293, 2437–2440.

Shim, S.-H., Duffy, T.S., Takemura, K., 2002. Equation of state of gold and its application to the phase boundaries near the 660-km depth in the mantle. Earth Planet. Sci. Lett. 203, 729–739.

Sinogeikin, S.V., Zhang, J., Bass, J.D., 2004. Elasticity of single crystal and polycrystalline $MgSiO_3$ perovskite by Brillouin spectroscopy. Geophys. Res. Lett. 31, L06620.

Speziale, S., Milner, A., Lee, V.E., Clark, S.M., Pasternak, M.P., Jeanloz, R., 2005. Iron spin transition in Earth's mantle. P. Natl. Acad. Sci. 102, 17918–17922.

Stackhouse, S., Brodholt, J.P., Price, G.D., 2007. Electronic spin trasitions in iron-bearing $MgSiO_3$ perovskite. Earth Planet. Sci. Lett. 253, 282–290.

Stixrude, L., Hemley, R.J., Fei, Y., Mao, H.K., 1992. Thermoelasticity of silicate perovskite and magnesiowüstite and stratification of the Earth's mantle. Science 257, 1099–1101.

Sturhahn, W., Jackson, J.M., Lin, J.-F., 2005. The spin state of iron in minerals of Earth's lower mantle. Geophys. Res. Lett. 32, L12307.

Takemura, K., 2001. Evaluation of the hydrostaticity of a helium-pressure medium with powder X-ray diffraction techniques. J. Appl. Phys. 89, 662–668.

Tsuchiya, T., 2003. First-principles prediction of the *P–V–T* equation of state of gold and the 660-km discontinuity in Earth's mantle. J. Geophys. Res. 108, 2462.

Tsuchiya, T., Wentzcovitch, R.M., da Silva, C.R.S., de Gironcoli, S., 2006. Spin transition in magnesiowüstite in Earth's lower mantle. Phys. Rev. Lett. 96, 198501.

Vanpeteghem, C.B., Zhao, J., Angle, R.J., Ross, N.L., Bolfan-Casanova, N., 2006. Crystal structure and equation of state of $MgSiO_3$ perovskite. Geophys. Res. Lett. 33, L03306.

Wittlinger, J., Fischer, R., Werner, S., Schneider, J., Schulz, H., 1997. High-pressure study of h.c.p. -argon. Acta Crystallogr. B53, 745–749.

Yeganeh-Haeri, A., 1994. Synthesis and re-investigation of the elastic properties of single-crystal magnesium silicate perovskite. Phys. Earth Planet. Inter. 87, 111–121.

Zhang, F., Oganov, A.R., 2006. Valence state and spin transitions of iron in Earth's mantle silicates. Earth Planet. Sci. Lett. 249, 436–443.